Reprinted from The Journal of Physical Chemistry, 1994, 98.

Theoretical Study on the Molecular and Dissociative Adsorptions of H_2 on a ZrO_2 Surface

H. Nakatsuji,*,†,‡,§ M. Hada,† H. Ogawa,† K. Nagata,† and K. Domen‡

Department of Synthetic Chemistry and Biological Chemistry, Faculty of Engineering, Kyoto University, Kyoto 606, Japan, Research Laboratory of Resources Utilization, Tokyo Institute of Technology, Midori-ku, Yokohama 227, Japan, and Institute of Fundamental Chemistry, 34-4 Takano Nishihiraki-cho, Sakyo-ku, Kyoto 606, Japan

Received: April 5, 1994; In Final Form: August 3, 1994[⊗]

The structures of molecularly and dissociatively adsorbed hydrogens on a ZrO_2 surface are studied by ab-initio SCF calculations for $Zr_3O_8(H_8)-H_2$ cluster embedded in an electrostatic potential representing the Madelung potential. The side-on and end-on molecular adsorption states on the Zr and O atoms, respectively, are calculated to have adsorption energies of 7.5 and 3.1 kcal/mol, and the heterolytic dissociation state is calculated with a heat of adsorption of 22.7 kcal/mol, while the experimental value is 8 kcal/mol. The IR frequencies of the H−H, Zr−H, and O−H stretching vibrations are calculated and compared with the experimental values. The reaction path for the dissociation of H_2 on the surface is calculated and the electronic mechanism of the dissociation is discussed. The calculated activation energy is 29.5 kcal/mol, while the experimental one is 10 kcal/mol. The mechanism for the chemisorption and dissociation of a hydrogen molecule on the ZrO_2 surface is discussed, and analysis of the electron density is presented.

1. Introduction

Spectroscopic investigations on the various hydrogen species chemisorbed on metal and metal-oxide surfaces have been performed in recent years.[1-5] On ZnO and ZrO_2 surfaces, the metal−H and O−H stretching frequencies have been observed and their behaviors have been examined by the IR spectroscopy.[1-3] However, the geometries of the adsorbed hydrogens and the electronic mechanism of the dissociative adsorption of a hydrogen molecule on the surface have not yet been clarified.

Previously, we have studied the electronic mechanisms for the dissociation of a hydrogen molecule over a ZnO surface using the ab-initio molecular orbital method.[6] We found that the electrostatic field of ZnO, represented as Zn^+ and O^-, directly interacting with H_2, polarized the homo (highest occupied molecular orbital) and the lumo (lowest unoccupied molecular orbital) of the hydrogen molecule. This causes the interaction between H_2 and ZnO to be favorable. We also investigated the role of the low-lying excited states along the reaction path and found that these are not important for the dissociation of a hydrogen molecule on a ZnO surface, i.e., only the ground state is involved in the chemisorption process.

We have previously studied hydrogen chemisorption on Pd[12] and Pt[13] surfaces, using correlated wave functions. We found that a hydrogen molecule dissociates into two atoms with a very low activation energy on the Pd surface and essentially without energy barrier on the Pt surface. The surface-excited state was found to play an important role on the Pt surface. The complete catalytic cycle for the hydrogenation of acetylene on the Pd surface has been reproduced theoretically.[14]

Kondo et al. reported the FT-IR experiment for the hydrogen molecule adsorbed on a ZrO_2 surface.[3] They assigned the observed peaks to three types of H−H vibrations and two types of Zr−H stretching vibrations, implying that three different molecular adsorption states and two different dissociative adsorption states are expected to exist on the surface. The suggested geometries are schematically shown below.

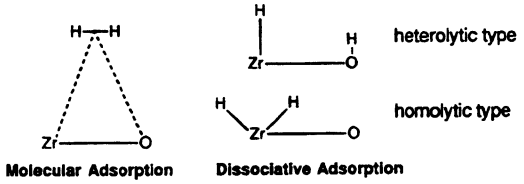

In the dissociative adsorption, two Zr−H bonds are formed in the homolytic dissociation, while Zr−H and O−H bonds are formed in the heterolytic case. In this paper, we theoretically study the chemisorption of hydrogen on a ZrO_2 surface. We study the geometries of molecularly and dissociatively adsorbed hydrogens on a ZrO_2 surface, and the reaction path for the dissociation of H_2 from the molecular adsoprtion state to the dissociative one. We also focus on the electronic mechanism of the molecular and dissociative adsorption of a hydrogen molecule on a ZrO_2 surface.

2. Method of Calculations

We have assumed that the structure of ZrO_2 surface is in the fluorite-type cubic geometry with the Zr−O distances of 2.23 Å.[7] As a prospective model for the ZrO_2 surface on which all types of adsorptions we are going to study in this paper are possible, we adopt the Zr_3O_8 cluster shown in Figure 1. This geometry is taken from the first and second layers of the ZrO_2-(110) surface. In this cluster, the central Zr and O atoms, marked by the asterisks, are connected to all the nearest-neighbor O and Zr atoms, respectively, and therefore offer the best approximation to the real surface atoms. For the capping of the artificial boundary valences, hydrogen atoms are put on the terminal Zr and O atoms as shown on the left-hand side of Figure 1. On the right-hand side, + and − signs show the point charges of +0.5 and −1.0 put on the Zr and O lattice positions, respectively, representing the electrostatic Madelung potential. The interactions between the terminal hydrogens and the point charges are not real; however, they do not affect the energetics

† Kyoto University.
‡ Tokyo Institute of Technology.
§ Institute of Fundamental Chemistry.
⊗ Abstract published in *Advance ACS Abstracts,* October 1, 1994.

0022-3654/94/2098-11840$04.50/0

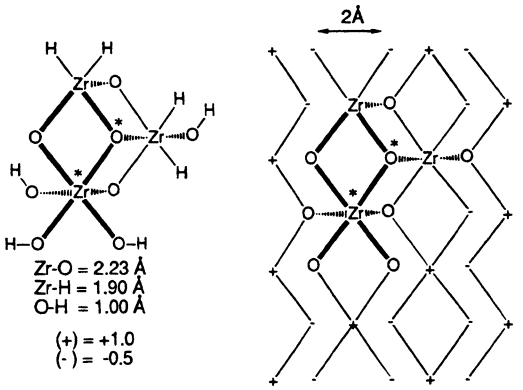

Figure 1. Cluster model for ZrO_2 surface with point charges on the crystal lattice (right) and with the terminal hydrogens (left). Two Zr atoms and four O atoms are on the first layer, and the rest are on the second layer. 111 point charges are put on the first and second layers. This picture does not show all the point charges used in this calculations. The Zr−H and O−H distances for capped hydrogens are 1.90 and 1.00 Å, respectively.

of the adsorption and the dissociation of H_2 because they are nearly constant throughout the processes. A hydrogen molecule, as an admolecule, is made to approach the central Zr−O (with the asterisks) from above. We performed a number of trial calculations to find the stable geometries of a hydrogen molecule and a hydrogen atom around the central Zr−O bond.

In our preliminary investigations we employed the small clusters ZrO_2 and Zr_3O_8, without the capping hydrogens. We found that both clusters were too reactive to reproduce reasonably the experimental heat of adsorption of H_2. The reaction of ZrO_2 with H_2 gives a stable ZrO_2H_2 molecule and is exothermic by 90 kcal/mol, while the experimental heat of adsorption of H_2 on the surface is about 8 kcal/mol.[3] The cluster size should be at least Zr_3O_8 for an adequate representation of the reactivity of the ZrO_2 surface. As the chemical interaction between hydrogen and surface is very local in nature for metal oxides, we think the adsorption is well described by the Zr_3O_8 cluster. The capping hydrogens are also necessary to lower the reactivity of the Zr_3O_8 cluster.

We carry out ab-initio RHF-SCF calculations for this H_2−$Zr_3O_8(H_8)$ system. For the central Zr atom, the valence double-ζ basis functions [2s2p2d] are used and the Kr-core is replaced by the effective core potential (ECP).[8] The [3s2p] functions[9] are used for the central O atom, and [2s] functions[9] plus their first derivatives[10] are used for the hydrogens approaching on the surface. The Hellmann−Feynman theorem is therefore satisfied for the forces acting on these hydrogens.[10] The reaction path and the optimized geometries are calculated based on the Hellmann−Feynman force. For the terminal Zr, O, and H atoms we use smaller bases: [1s1p1d] + ECP(Kr-core),[8] STO-6G, and STO-3G,[11] respectively. To mimic the Madelung potential, the 111 point charges of 1.0 and −0.5 are placed at the Zr and O lattice sites, respectively. The sum of the point charges is zero. We add two excess electrons to the cluster because the cluster has excess two oxygen atoms in comparison with the natural component of ZrO_2. Thus, we use $[Zr_3O_8(H_8)-H_2]^{2-}$ + 111 point charges as a model system of the ZrO_2 surface plus adsorbed H_2 molecule.

3. Stable Geometries of the Adsorbed Hydrogens

All the stable geometries of H_2 are found around the central Zr−O bond of $Zr_3O_8(H_8)$ and summarized in Figure 2 and Table 1. The molecularly adsorbed structures are shown in Figure 2a,b. The relaxation of the Zr_3O_8 cluster is not considered in this paper. We found two types of molecular hydrogens adsorbed on the cluster: one is the side-on structure on the Zr atom shown in Figure 2a, and the other is the end-on structure on the O atom shown in Figure 2b. The third type of the molecularly adsorbed H_2 suggested by Kondo et al.[3] could not be found in the present investigation. The end-on structure on Zr and the side-on structure on O are both unstable as they spontaneously give either a free H_2 or the stable adsorbed H_2 shown in Figure 2a,b. The H−H distance of H_2 on Zr is 0.738 Å and that on O is 0.737 Å; they are essentially the same as that of a free H_2 molecule, 0.731 Å. The heats of adsorption are 7.5 and 3.1 kcal/mol for the types (a) and (b), respectively. The Zr site is favorable to the O site for molecular adsorption.

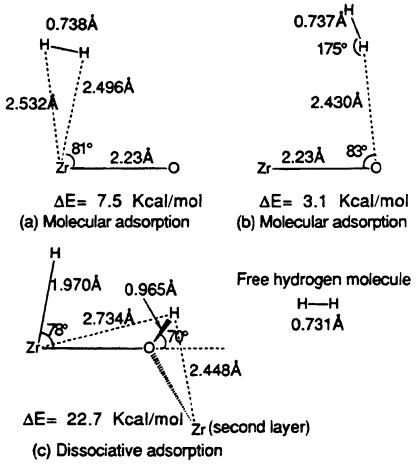

Figure 2. Optimized geometries and optimized geometrical parameters for the two types of molecularly adsorbed hydrogen molecule (a) and (b) and one type of dissociative adsorption (c). ΔE is the stabilization energy relative to a free H_2. The H−H distance of the free H_2 is 0.731 Å at the same level of calculation.

TABLE 1: Geometries of the Molecularly and Dissociatively Adsorbed Hydrogens Shown in Figure 2 (Å)[a]

	H (left)			H (right)		
state	*X*	*Y*	*Z*	*X*	*Y*	*Z*
a	0.0	0.375	2.468	0.0	−0.362	2.507
b	0.291	2.291	2.412	0.104	2.277	3.125
c	0.693	2.583	0.571	−0.008	0.413	1.927

[a] The coordinates of the central Zr and O atoms are Zr (0.0, 0.0, 0.0) and O (0.0, 2.229, 0.0).

The geometry of the dissociatively adsorbed hydrogen is shown in Figure 2c. This is the heterolytic dissociation type with Zr−H and O−H bonds formed. The O−H bond is largely inclined toward the Zr atom on the second layer, as shown in Figure 2c. The dissociatively adsorbed hydrogens are much more stable that the molecularly adsorbed hydrogens shown in Figure 2a,b. The stabilization energy is 22.7 kcal/mol, while the experimental heat of adsorption is 8 kcal/mol.[3] The homolytic fission on the Zr atom, as suggested by Kondo et al., is shown not to occur on the present Zr_3O_8 cluster.

4. IR Frequencies of the Adsorbed Hydrogens

Table 2 shows the calculated frequencies for the H−H, Zr−H, and O−H stretching vibrations of the adsorbed hydrogens shown in Figure 2. These frequencies are calculated by assuming that the Zr and O atoms are fixed during the vibrations.

The frequencies for the H−H stretching vibrations of the molecularly adsorbed hydrogens are shown on the left-hand side of the table. The frequency for the side-on structure of type (a) of Figure 2 is smaller than that for the end-on structure of type (b), showing that the H−H bond on the Zr atom is

TABLE 2: Vibrational Frequencies of the Hydrogens Adsorbed on a ZrO_2 Surface (cm^{-1})

				dissociative adsorption			
	molecular adsorption (H-H)			Zr−H[b]		O-H[b]	
state[a]	calcd	exptl[c]	state	calcd	exptl[c]	calcd	exptl[c]
		3996	c	1810	1562	3310	3663
a	4302	4031					
b	4324	4054					

[a] States a, b, and c are defined in Figure 2. [b] Frequencies are calculated by assuming that the Zr and O atoms are fixed during the vibrations. [c] Reference 3.

weakened more than that on the O atom. This result corresponds to the fact that the stabilization energy for the adsorption type (a) is larger than that for type (b). The calculated band gap of the H−H stretching (22 cm^{-1}) is compared with the experimental values (35 or 23 cm^{-1}), which suggests that the two calculated frequencies are assigned to the energetically higher bands: 4031 and 4054 cm^{-1}. This assignment also agrees with the experimental suggestion that the middle band, 4031 cm^{-1}, is due to the precursor state for the dissociation process,[3] as discussed in the next section. The calculated frequencies for the H−H stretching vibrations are overestimated by about 270 cm^{-1} in comparison with the experiment. This overestimation is a general tendency of the Hartree−Fock method for stretching vibrational frequencies.

The vibrational frequencies of the Zr−H and O−H stretching vibrations for the dissociatively adsorbed hydrogen atoms are shown on the right-hand side of Table 2. The Zr−H stretching vibrational frequency, 1810 cm^{-1}, is smaller than the O−H one, showing that the Zr−H bond is significantly weaker than the OH bond. The calculated H−H frequencies are overestimated by 250 cm^{-1} relative to the experiment. The O−H vibrational frequency, however, is smaller by 250 cm^{-1} than the experimental values. This suggests that the calculated adsorption geometry is different from the experimentally observed one. This is because the hydrogen on the O atom interacts not only with the O atom but also with the Zr atoms on the second layer, as shown in the optimized geometry given in Figure 2c. In contrast, experimentally observed hydrogen on the O site (3663 cm^{-1}) seems to only interact with that oxygen atom because the frequency of the normal O−H stretching vibration of organic molecules is 3200−3600 cm^{-1}.

5. Dissociative Adsorption Pathway

Figure 3 shows the assumed reaction path from the molecular adsorption state to the dissociative adsorption state. Figure 4 shows the corresponding energy diagram. The geometries 1 and 8 in Figure 3 correspond to the stable structures of the molecular and dissociative adsorptions shown in parts a and c of Figure 2, respectively. The molecularly adsorbed hydrogen on the Zr atom in Figure 2a is suitable as the precursor state for the dissociation because the adsorption energy on Zr is larger than that on O, as shown in Figure 2.

The points numbered 2−7 are determined in the following manner, and their explicit coordinates are given in Table 3. We first assume the hydrogen molecule at number 1 moves on the circle around the Zr atom with fixed H−H distance. The geometries 2 and 3 are on this path. This path is reasonable because the energy change is very small as shown in Figure 4 (numbers 1−3). At number 3 the hydrogen molecule is located above the center of the Zr−O bond. After number 3, the hydrogen is forced to approach the surface with the H−H distance elongating. For numbers 4 and 5 we assume that the right hydrogen approaches the oxygen atom, keeping the Zr−H

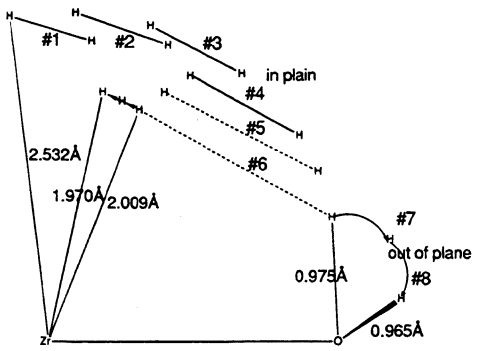

Figure 3. Assumed and partially optimized reaction path for the dissociation of a hydrogen molecule on a $Zr_3O_8(H_8)$ cluster. The geometries numbered 1, 6, and 8 are optimized. The left hydrogen at numbers 4 and 5 is optimized with fixing the right hydrogen. The hydrogen atoms at numbers 1−6 are fixed on the plane vertical to the surface and including the Zr−O bond.

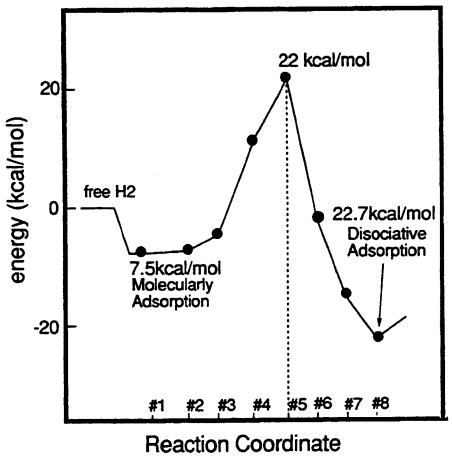

Figure 4. Potential energy along the path of the dissociation of a hydrogen molecule on a $Zr_3O_8(H_8)$ cluster shown in Figure 3.

TABLE 3: Reaction Path for the Dissociation of a Hydrogen Molecule on ZrO_2 (Å)

	H (left)			H (right)		
geometry[a]	X	Y	Z	X	Y	Z
1	0.0	0.375	2.468	0.0	−0.362	2.507
2	0.0	0.915	2.307	0.0	0.211	2.523
3	0.0	1.392	2.037	0.0	0.781	2.435
4	0.0	1.863	1.587	0.0	1.100	2.000
5	0.0	2.043	1.272	0.0	0.838	1.963
6	0.0	2.223	0.958	0.0	0.576	1.925
7	0.347	2.406	0.883	0.0	0.494	1.926
8	0.693	2.583	0.571	−0.008	0.413	1.927

[a] The geometries numbered 1−8 are depicted in Figure 3 and the coordinates of the central Zr and O atoms are Zr (0.0, 0.0, 0.0) and O (0.0, 2.229, 0.0).

distance constant, and that the left and the right hydrogens are in the same plane. The position of the left hydrogen is optimized at each step at numbers 4 and 5. At number 6 the positions of both hydrogens are optimized in the plane including Zr, O, and hydrogens. The geometry 8 is the stable geometry shown in Figure 2c, and the geometry 7 is obtained by a simple interpolation between numbers 6 and 8, with the OH distance taken to be 0.970 Å.

The energy maximum along this reaction path exists around number 5. The energy of number 5 is 29.5 kcal/mol relative to the energy level of the molecularly adsorbed state (number 1). This value gives the upper limit for the activation energy of

TABLE 4: Gross Atomic Charges of H_2 and the ZrO_2 Surface

geometry no.[b]	H (left)	H (right)	Zr	O
0[a]	0.00	0.00	+1.48	−1.12
1	+0.06	−0.02	+1.41	−1.13
2	+0.05	−0.04	+1.43	−1.14
3	+0.08	−0.08	+1.46	−1.14
4	−0.22	+0.13	+1.50	−1.13
5	−0.35	+0.37	+1.46	−1.06
6	−0.34	+0.37	+1.26	−1.01
8	−0.31	+0.38	+1.22	−1.08
e[c]	0.31	−0.29	1.47	−1.15

[a] Geometry 0 corresponds to H_2 molecule and free cluster. [b] Geometries numbered 1−8 and the left and right hydrogens are defined in Figure 3. [c] Geometry e is the end−on adsorption geometry of H_2 on O shown in Figure 2b.

this reaction, and the transition state of the dissociation reaction must exist near number 5. After number 6 the hydrogen atom, interacting with the oxygen atom on the right-hand side of Figure 3, departs from the plane. At number 8 two hydrogens reach the most stable dissociative adsorption sites on Zr and O, forming the Zr−H and O−H bonds.

In summary, the hydrogen molecule adsorbed on the Zr atom moves on the adsorption radius of the Zr atom to the center of the Zr−O bond and then approaches to the surface, dissociating and forming the Zr−H and O−H bonds. The calculated dissociation barrier is 22 kcal/mol, relative to the free system, and the calculated heat of adsorption is 22.7 kcal/mol, while the experimental value is about 10 kcal/mol.[3]

6. Electronic Mechanism for Molecular and Dissociative Adsorptions

We found two types of molecularly adsorbed hydrogen as explained in section 3 and in Figure 2. The main orbital interactions involved are sketched as follows.

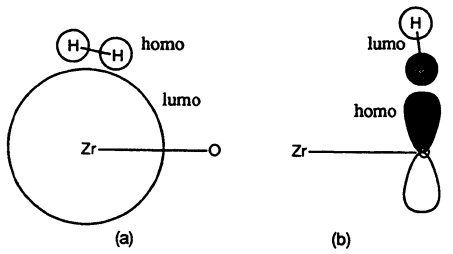

(a) The homo (highest occupied molecular orbital) of the hydrogen molecule interacts with the lumo (lowest unoccupied molecular orbital) of the surface, which is mainly the 5s orbital of Zr, and some electron is transferred from the hydrogen molecule to the surface. This interaction is the origin of the molecular adsorption of type (a) shown in Figure 2. The side-on geometry is a natural consequence of this orbital interaction. (b) The homo of the surface, which is mainly the 2p orbital of O, interacts with the lumo of the hydrogen molecule. This interaction favors the end-on geometry of H_2 on the O atom as shown in Figure 2b. The side-on geometry on the O atom is expected to be less stable, because the interaction (b) disappears by the orbital symmetry.

Table 4 shows the gross atomic charges of H_2 and the ZrO_2 surface. At the side-on geometry number 1, the charge polarization of the adsorbed H_2 is very small, while at the end-on geometry (e), it is large. This is easily understood from the nature of the homo−lumo interaction illustrated in the above figure.

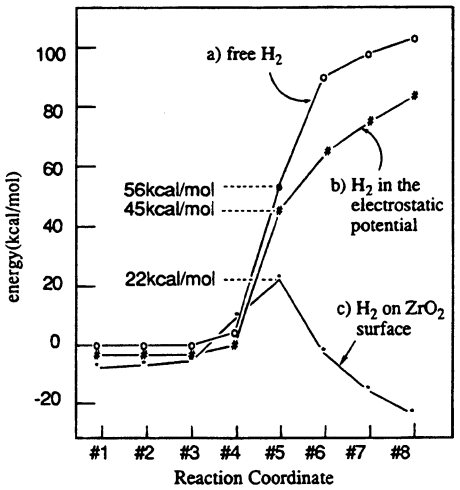

Figure 5. Potential energies along the dissociation path of the hydrogen molecule in different environments. (a) Free hydrogen molecule; (b) hydrogen molecule in the electrostatic field due to the point charges put on the lattice sites of the ZrO_2 surface instead of the actual Zr and O atoms; (c) hydrogen molecule interacting with the $Zr_3O_8(H_8)$ cluster and the point charges surrounding the cluster (the model of the surface adopted in this paper). The definitions of the reaction coordinates (numbers 1−8) are shown in Figure 3.

Next, we study the dissociation mechanism of H_2 on the ZrO_2 surface. Since the Zr−O bond is essentially ionic, the surface is charge polarized as seen from the Mulliken analysis in Table 4. Roughly, Zr is +1.4 and O is −1.1. In the previous study on the H_2 chemisorption on the ZnO surface,[6] we have shown the important role of this charge polarization in lowering the activation barrier. We therefore examine the effect of this electrostatic potential on the reaction barrier.

Figure 5 shows the potential energy curves along the dissociation pathway shown in Figure 3 for three different cases. They are (a) the free hydrogen molecule, (b) the hydrogen molecule in the electrostatic field due to the point charges put on the lattice potentials of the ZrO_2 surface, instead of the actual Zr and O atoms (the charges are +1.0 and −0.5 for Zr and O, respectively), and (c) the hydrogen molecule on the ZrO_2 surface studied in this paper. In case (a) we neglect the H_2−surface interaction and case (b) shows the effect of the electrostatic field alone. In cases (a) and (b) the potential curves are calculated by the full-CI method, because the potential curve for the dissociation of a free H_2 cannot be obtained by the Hartree−Fock method. The potential curve for case (c) is identical with the one shown in Figure 4, which is obtained at the HF level. Therefore the effect of the surface may be underestimated when we compare curve (c) with curves (a) and (b) in Figure 5.

In the initial stage, numbers 1−3, the electrostatic field does not affect H_2: cases (a) and (b) differ by only 2−3 kcal/mol. The effect of the actual surface is 7−4 kcal/mol. After passing number 4, these effects increase dramatically. At the transition state number 5, case (c) is lower than case (a) by 34 kcal/mol, showing the catalytic activity of the ZrO_2 surface. Here, the electrostatic field effect is estimated to be 11 kcal/mol, and the rest, 23 kcal/mol, reflects the other electronic interaction between H_2 and the surface. These effects increase as the dissociation of H_2 proceeds, numbers 6−8, as seen from Figure 5.

The electrostatic effect is actually larger than the direct effect of ~11 kcal/mol at number 5: the following indirect effect depicted in Figure 6 is expected to be important. The charge

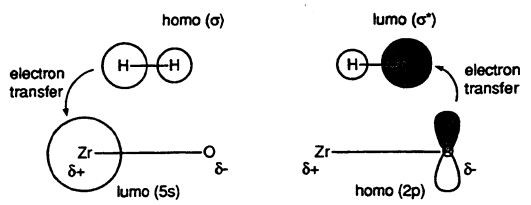

Figure 6. Schematic pictures of the homo–lumo interactions between H_2 and the surface assisted by the charge polarization of the ZrO_2 surface.

polarization of the ZrO_2 surface, Zr^+-O^-, directly interacting with H_2 works to polarize the homo and lumo of H_2. The homo is polarized toward Zr and consequently the lumo is polarized toward O. The former makes the H–H binding energy smaller, which is the origin of the lowering of ~11 kcal/mol at number 4. Moreover, this polarization facilitates the homo–lumo and back homo–lumo interactions between H_2 and the ZrO_2 surface. Namely, the lumo of the surface, 5s orbital of Zr, interacts more easily with the homo of H_2, and the homo of the surface, the 2p orbital of O perpendicular to the surface, interacts more easily with the lumo of H_2 than the case without charge polarization. This indirect electrostatic effect would be an important part of 23 kcal/mol at number 4. After passing the transition state, this interaction becomes larger and larger, the H–H bond is broken, and the nature of the bonding becomes like Zr^+-H^- and O^-H^+.

We have also pointed out the importance of the above direct and indirect electrostatic effects for the H_2 chemisorption on the ZnO surface.[6] We believe that the effect depicted in Figure 6 is commonly important for chemisorptions on metal oxide surfaces.

Table 4 shows the gross atomic charges of the two hydrogen atoms calculated by the Mulliken population analysis. The left and right H's are defined in Figure 3. For numbers 1–3, the left H has a positive charge and the right H has a negative charge. At number 4 the charge of the left H suddenly changes to negative, while that of the right H becomes positive. This charge polarization indicates that the hydrogen molecule starts to interact with the Zr and O atoms. This charge polarization, which is explained in Figure 6 by the polarization of the σ and σ^* orbitals of H_2, becomes gradually larger from number 4, and finally the two hydrogens have the charge polarizations understood as $Zr^{\delta+}-H^{\delta-}$ and $O^{\delta-}-H^{\delta+}$. The H atom dissociatively adsorbed on Zr would react as a hydride, while the H atom adsorbed on O would react as a proton, which is discussed in the next section.

7. Reactivity of the Dissociatively Adsorbed Hydrogens

We are interested in the reactivities of the dissociatively adsorbed hydrogens, although they are located at comparably stable sites on the surface, as studied in the above sections. We examined the mo's of the system in the homo–lumo region and found that the Zr–H bonding and O–H antibonding orbitals appear in these region when the hydrogen molecule is dissociatively adsorbed on the surface. The Zr–H bonding orbital which consists chiefly of 4d of Zr and 1s of H becomes the next homo. The next lumo has O–H antibonding character, though the weight is relatively small. Therefore, the hydrogens on the Zr and O atoms are expected to be reactive to electrophiles and nucleophiles, respectively. In the attack of the electrophile an electron is donated from the Zr–H bond which is then weakened. The electrophile may subtract H^- from the surface. The O–H bond is weakened by the nucleophilic attack. When the Zr–H and O–H bond are weakened, the electrophilic and nucleophilic reactions are further accelerated. No other appreciable changes of the orbitals on the ZrO_2 surface

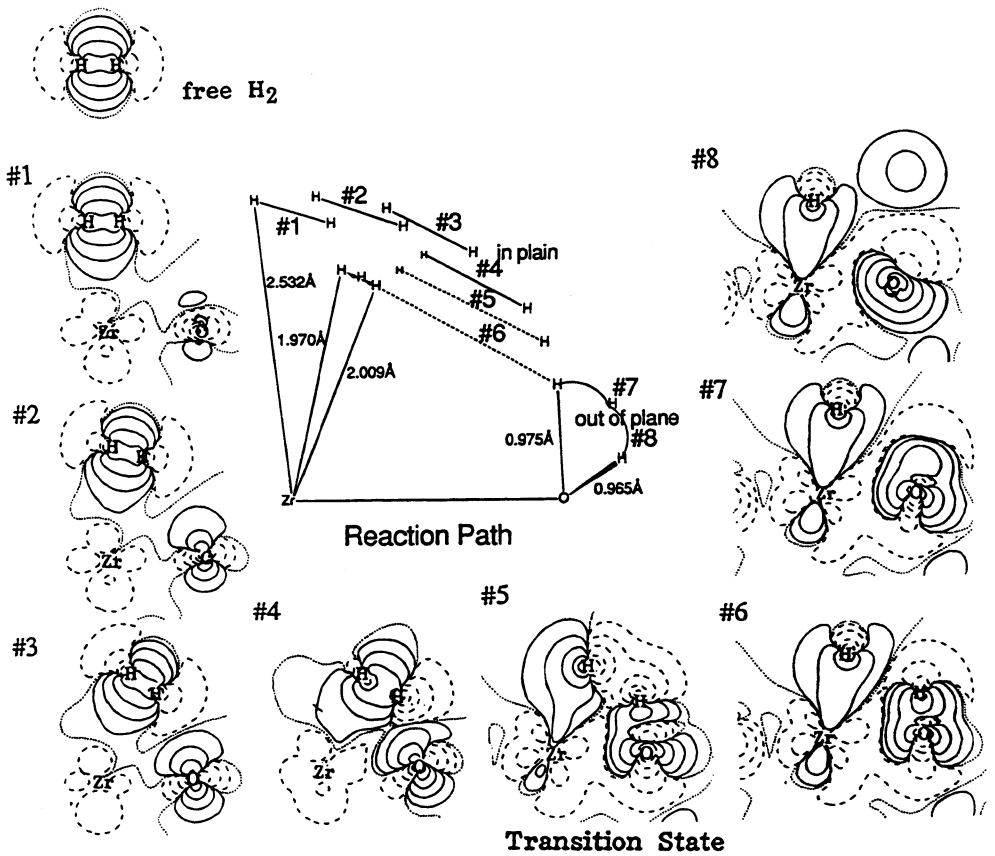

Figure 7. Contour maps of the electron density difference along the dissociation reaction path shown at the center of this figure. The definitions of the density difference and the coordinates numbered 1–8 are given in the text and in Figure 3, respectively.

are observed by the adsorption of the hydrogen, suggesting that the surface is stable when a hydrogen molecule is adsorbed on the surface. Needless to say that in the molecularly adsorbed states, the bonding and antibonding mo's of H_2 occur deep in the occupied mo's and high above the lumo levels, respectively.

8. Analysis of Electron Density

Figure 7 shows the contour maps of the electron density difference along the dissociation path. The definition of the electron density difference $\Delta\varrho$ is

$$\Delta\varrho = \varrho(\text{cluster}-H_2) - \varrho(\text{cluster}) - \varrho(H) - \varrho(H),$$

where $\varrho(M)$ is the electron density of the system M. In the initial stage, numbers 1−3, the bonding nature of the adsorbed hydrogen molecule is kept, though the electron density is polarized toward the surface. At number 4, the electron density of the hydrogen molecule is polarized toward the left H atom as explained in Figure 6. This is reflected in the change in the gross atomic charges of the hydrogens shown in Table 4. The Zr−H (left) and O−H (right) bonds are formed gradually. At transition state number 5, the Zr−H and O−H bonds are clearly formed and the H−H bond is completely broken. There occurs a sudden reorganization of electron density between numbers 4 and 5. At number 6, the Zr−O and O−H bonds become stronger than those of number 5. The adsorbed hydrogens are in the most stable geometry if they are restricted on the vertical plane including the Zr and O atoms. At numbers 7 and 8, the H (right) departs from the vertical plane. At number 8, the Zr−O bond of the surface is weakened, and the O atom tends to form a new bond with the Zr atom on the second layer.

9. Summary

We have studied the molecular and dissociative adsorptions of H_2 on a ZrO_2 surface using the cluster model $[Zr_3O_8(H_8)-H_2]^{2-}$ embedded in 111 point charges put on the crystal lattice positions of the ZrO_2 crystal. We may summarize the results as follows.

(i) Two stable geometries are calculated for the molecularly adsorbed hydrogens: one is side-on above the Zr atom and the other is end-on above the O atom, with heats of adsorption 7.5 and 3.1 kcal/mol, respectively. These structures correspond to the two of the three types of the molecularly adsorbed hydrogens suggested experimentally.[3] The end-on adsorption on Zr and the side-on adsorption on O are unstable.

(ii) One stable geometry is obtained for the dissociatively adsorbed hydrogens. It is the heterolytic adsorption on Zr and O giving Zr−H and O−H bonds. The calculated heat of adsorption is 22.7 kcal/mol, which is larger than the experimental value of 8 kcal/mol. The homolytic dissociation on the Zr atom suggested previously[3] is unstable in the present calculations.

(iii) The reaction path from the molecularly adsorbed state on the Zr atom to the dissociatively adsorbed state on the Zr and O atoms is calculated (Figure 3). The calculated heat of activation is 22 kcal/mol, while the experimental value is 10 kcal/mol.

(iv) The origin of the molecular adsorption of H_2 at the Zr site is the H_2 homo (σ mo)−Zr lumo (5s) interaction and that at the O site is the O homo (2p mo perpendicular to the surface)−H_2 lumo interaction, which make respectively the side-on geometry on Zr and the end-on geometry on O favorable.

(v) In the dissociation process of H_2, the polarization of the homo and lumo of H_2 due to the charge polarization Zr^+-O^- on the surface play an important role to facilitate the interaction between H_2 and the metal oxide surface. This is common to the H_2 dissociation on a metal oxide surface including ZnO studied previously.[6]

(vi) The dissociatively adsorbed H on Zr is reactive for electrophilic attack, while that on O is reactive for the nucleophilic attack.

Acknowledgment. Part of the calculations have been carried out with the computers at the Data Processing Center of Kyoto University and at the Institute of Molecular Science. We thank the IMS computer center for the grants of computing time. This study has partially been supported by the Grant-in-Aid for Scientific Research from the Japanese Ministry of Education, Science, and Culture, and by CIBA-GEIGY Foundation (Japan) for the Promotion of Science.

References and Notes

(1) Hussain, G.; Sheppard, N. *J. Chem. Soc. Faraday Trans.* **1990**, *86*, 1615, and references therein.
(2) Onishi, T.; Abe, H.; Maruyama, K.; Domen, K. *J. Chem. Soc. Chem. Commun.* **1985**, 617.
(3) (a) Kondo, J.; Domen, K.; Maruyama, K.; Onishi, T. *J. Chem. Soc. Faraday Trans.* **1990**, *86*, 397. (b) Kondo, J.; Domen, K.; Maruyama, K.; Onishi, T. *Chem. Phys. Lett.* **1992**, *188*, 443.
(4) Lamotte, J.; Lavally, J. C. *J. Chem. Soc. Faraday Trans. I* **1985**, *81*, 215.
(5) Coluccia, S.; Boccuzzi, F.; Ghiotti, G.; Morterra, C. *J. Chem. Soc. Faraday Trans. I*, **1982**, *78*, 2111.
(6) Nakatsuji, H.; Fukunishi, F. *Intern. J. Quantum Chem.* **1992**, *42*, 1101.
(7) *Handbook of Chemistry and Physics*; CRC Press: Cleveland, OH, 1984−1985.
(8) Hay, P. J.; Wadt, W. R. *J. Chem. Phys. Lett.* **1980**, *75*, 270.
(9) Dunning, T. H., Jr. *J. Chem. Phys.*, **1970**, *53*, 2823.
(10) (a) Nakatsuji, H.; Kanda, K.; Yonezawa, T. *Chem. Phys. Lett.* **1980**, *75*, 340. (b) Nakatsuji, H.; Kanda, K.; Hada, M.; Yonezawa, T. *J. Chem. Phys.* **1982**, *77*, 3109; *Chem. Phys. Lett.* **1983**, *95*, 573.
(11) Hehre, W. J.; Stewart, R. F.; Pople, J. A. *J. Chem. Phys.* **1969**, *51*, 2657.
(12) (a) Nakatsuji, H.; Hada, M.; Yonezawa, T. *J. Am. Chem. Soc.* **1985**, *107*, 8264. (b) Nakatsuji, H.; Hada, M.; Yonezawa, T. *J. Am. Chem. Soc.* **1987**, *109*, 1902.
(13) Nakatsuji, H.; Matsuzaki, Y.; Yonezawa, T. *J. Chem. Phys.* **1988**, *88*, 5759.
(14) Nakatsuji, H.; Hada, M.; Yonezawa, T. *Surf. Sci.* **1987**, *185*, 319.